

GREAT DESIGNS IN **STEEL**

FRACTURE DETECTION IN THE VDA 238-100 TIGHT RADIUS BEND TEST FOR SEVEN AUTOMOTIVE STEELS

A collaborative project between Honda R&D Americas, AISI Automotive Program, Bowman Precision Tooling, and the University of Waterloo

University of Waterloo

Jacqueline Noder, Prof. Butcher

Honda R&D Americas, LLC

Jim Dykeman, Skye Malcolm

UNIVERSITY OF WATERLOO RESEARCH TEAM

Cliff Butcher – Assistant Professor

Jacqueline Noder – PhD Candidate

Edward Gutierrez – MASc Student

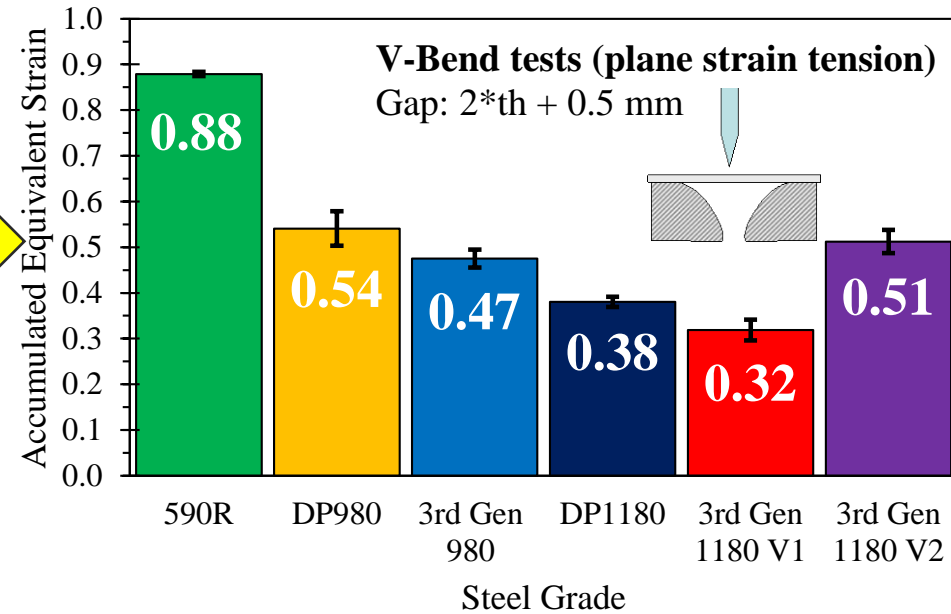
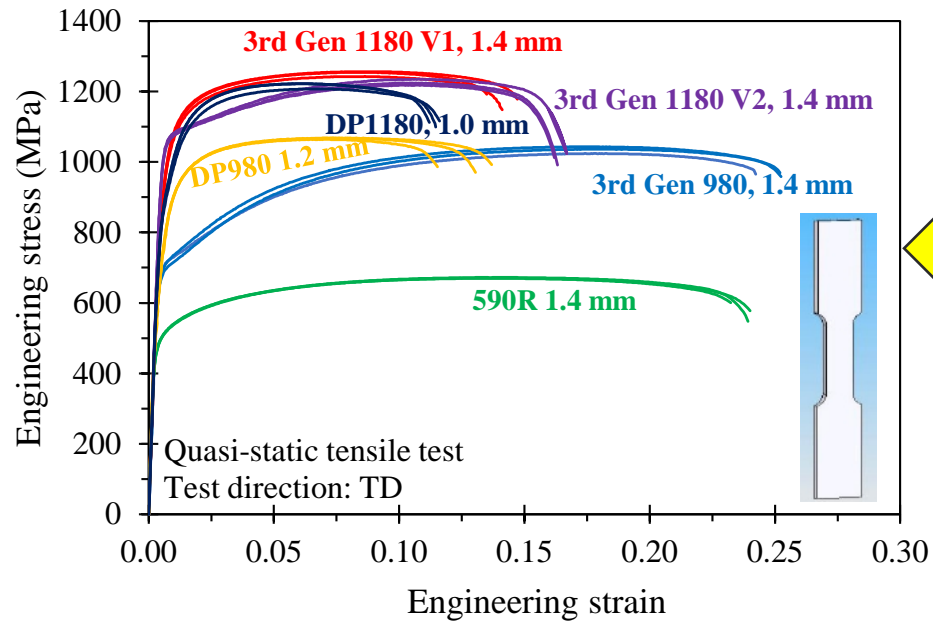
Nicholas Aydemir – MASc Student

Amir Zhumagulov – Research Associate

MOTIVATION

- Develop CAE predictive capabilities for formability and crash performance of 3rd Gen AHSS (980 and 1180 tensile strength) structural components
- Confirm capability on a mid-size SUV B-pillar design*

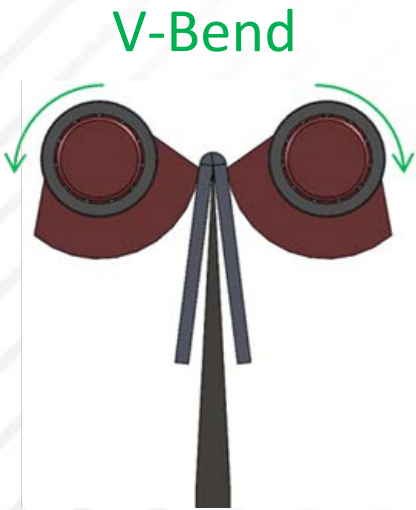
* *Separate GDIS presentation: “Formability and fracture Validation of 3rd Gen steels”, Prof. Cliff Butcher*



Tensile tests provide only limited correlation with local material behavior for structural components

OBJECTIVES

VDA 238-100 tight radius bend test is simple and fast to perform but has limitations for ductile alloys or thin sheet



Load drop as unique fracture metric
Occasional reduction in punch force without material rupture

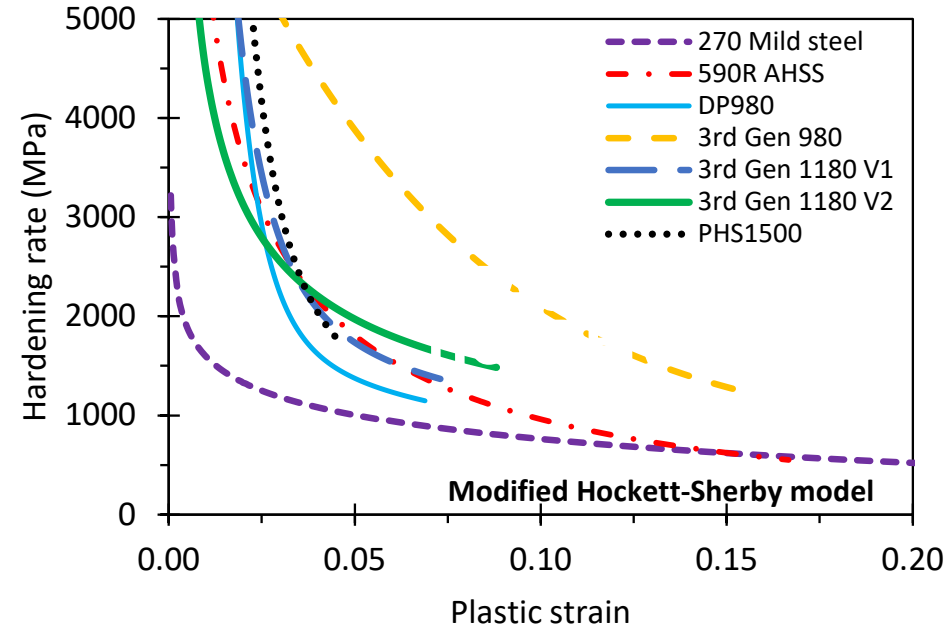
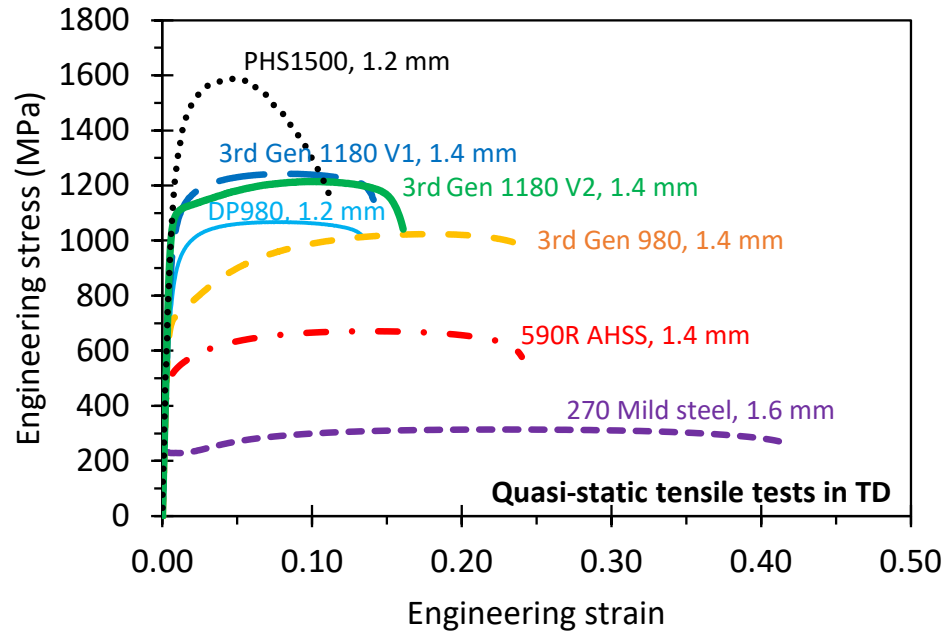
Pre-straining of specimen prior to bend operation
Represents a non-proportional strain path which affects subsequent material behavior

Objective: Identify alternative fracture detection method to reliably determine material failure from inconclusive results in the V-Bend test

Experimental V-Bend study is discussed in separate GDIS presentation “Effect of AHSS Gauge and Punch Radius in Three-point Bending”, Kenneth Cheong

MATERIAL SELECTION

Seven automotive steel grades with varying ductility levels were considered



	Yield Stress (0.2% offset) (MPa)	Ultimate Tensile Stress (MPa)	Uniform Elongation UE (%)	Total Elongation TE (%)
270 Mild steel, 1.6 mm	256 (±1)	311 (±2)	31.1 (±2.8)	43.2 (±1.0)
590R AHSS, 1.4 mm	490 (±2)	671 (±1)	13.7(±0.1)	23.8 (±0.4)
3rd Gen. 980, 1.4 mm	681 (±8)	1033 (±10)	18.0 (±0.5)	24.9 (±0.6)
3rd Gen. 1180 V2, 1.4 mm	1047 (±10)	1219 (±5)	10.3 (±0.3)	16.2 (±0.1)
DP980, 1.2 mm	735 (±2)	1065 (±3)	7.8 (±0.2)	14.1 (±0.6)
3rd Gen. 1180 V1, 1.4 mm	950 (±12)	1251 (±8)	8.4 (±0.2)	13.7 (±0.5)
PHS1500, 1.2 mm	1144	1571	5.5	11.0

High ductility

Moderate ductility

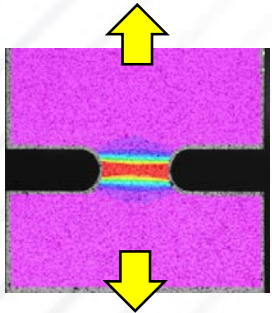
Low ductility

PLANE STRAIN FRACTURE TESTS

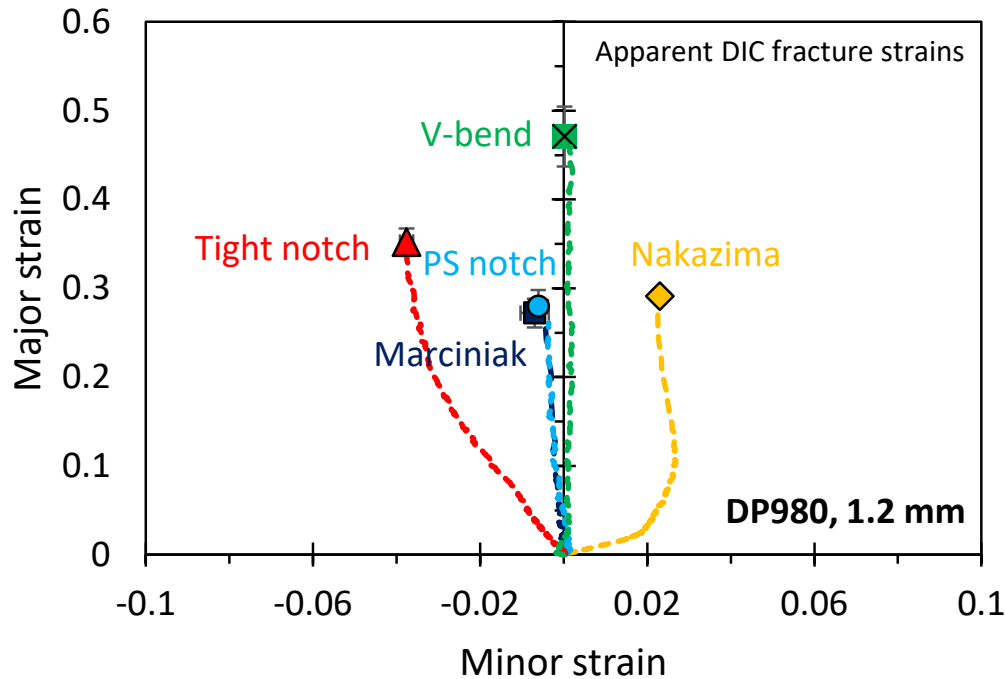
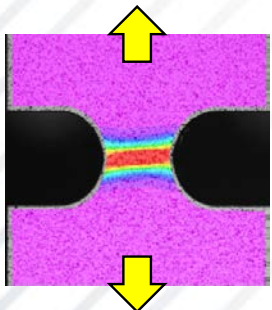
All tests induce failure under plane strain tension

Linearity of strain path and magnitude of apparent fracture strain greatly vary

Plane strain notch

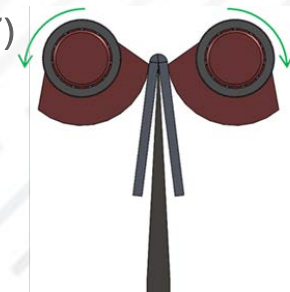
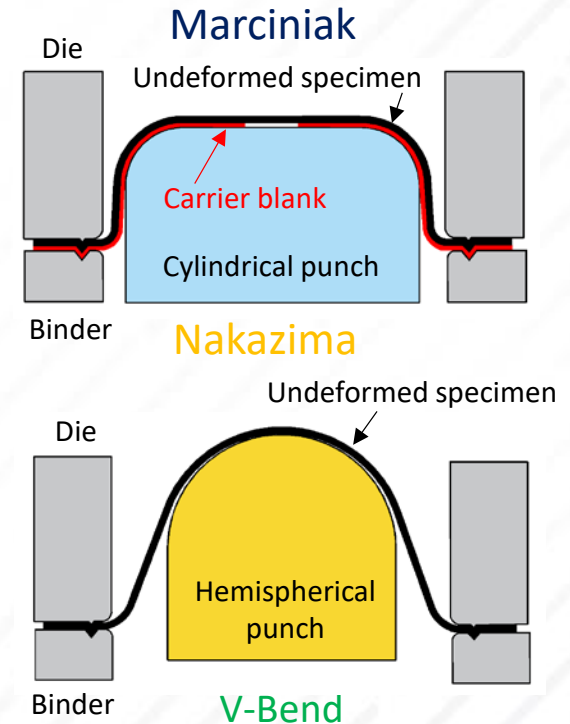


Tight notch



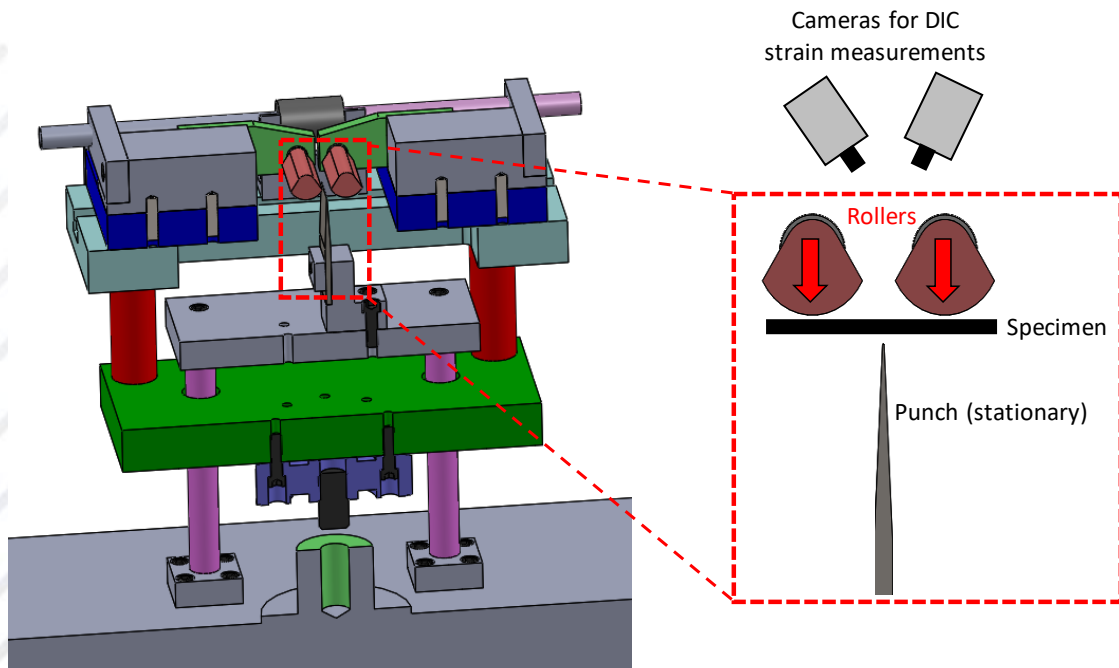
Note: Rupture strains in necking-induced tests can be measured post-test (GDIS 2017)

Only V-bend provides approximate proportional loading – Necking instability is suppressed

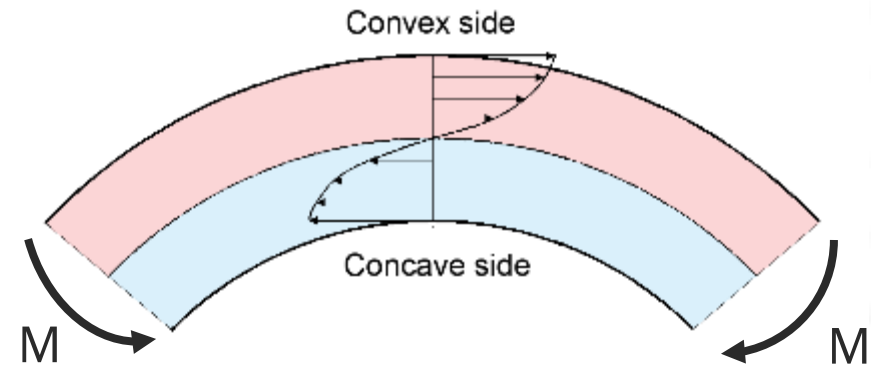


V-BEND TEST FRAME

Test frame utilized for this study was inverted and equipped with DIC
Fracture strain can be retrieved from the experiment without inverse FEA



Material layers above neutral axis are in plane strain tension

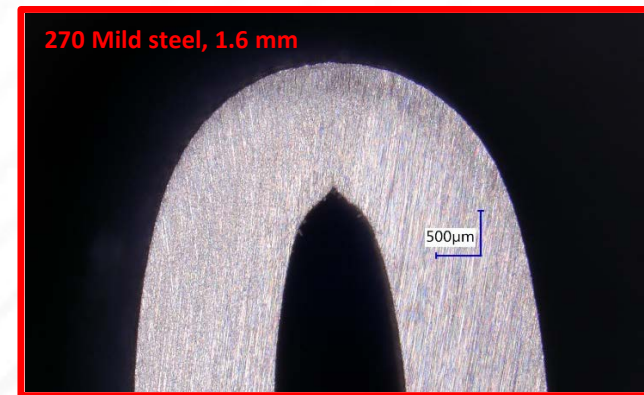
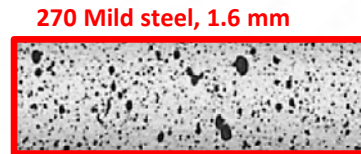
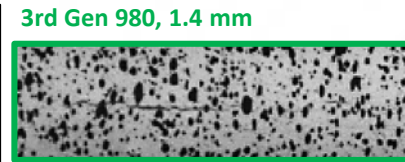
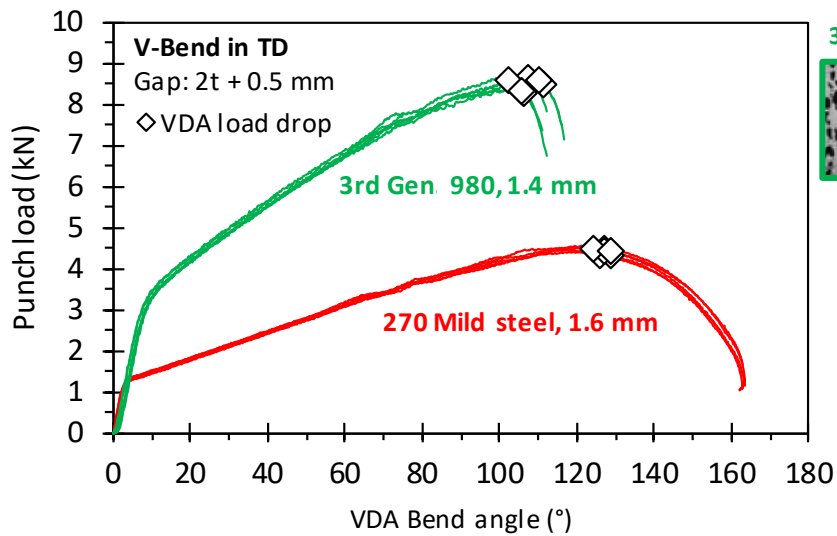


Material layers below neutral axis are in plane strain compression

Severe through-thickness stress-strain gradient suppresses necking

CHALLENGES WITH V-BEND TEST

VDA 238-100 recommends failure identification from reduction in punch force

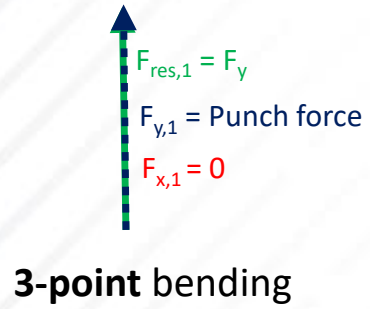


Clear signs of fracture for the 3rd Gen 980

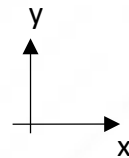
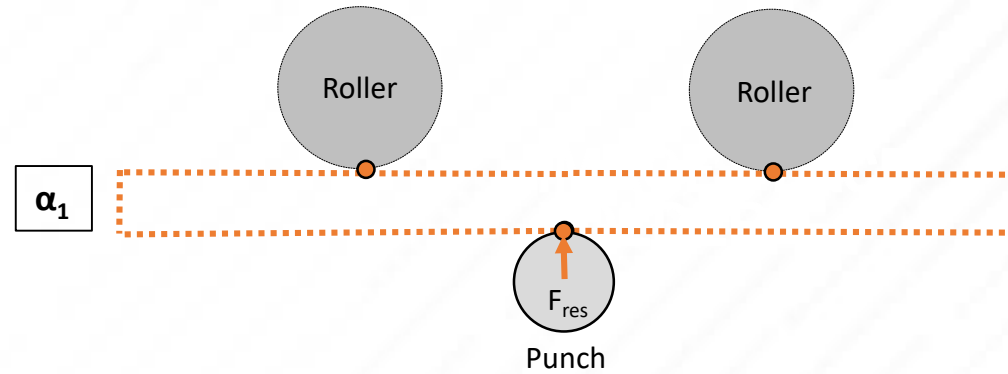
No fracture on convex specimen side for the 270 Mild steel → “False positive”

MECHANICS OF V-BEND TEST

What causes the load to reduce in the absence of fracture?

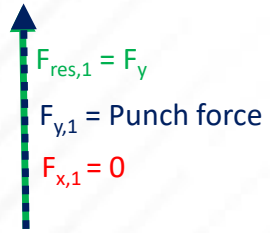


α_1



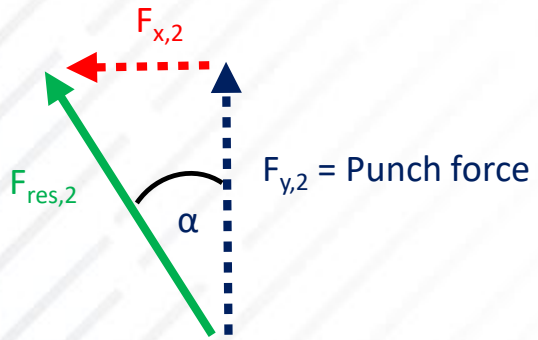
MECHANICS OF V-BEND TEST

What causes the load to reduce in the absence of fracture?



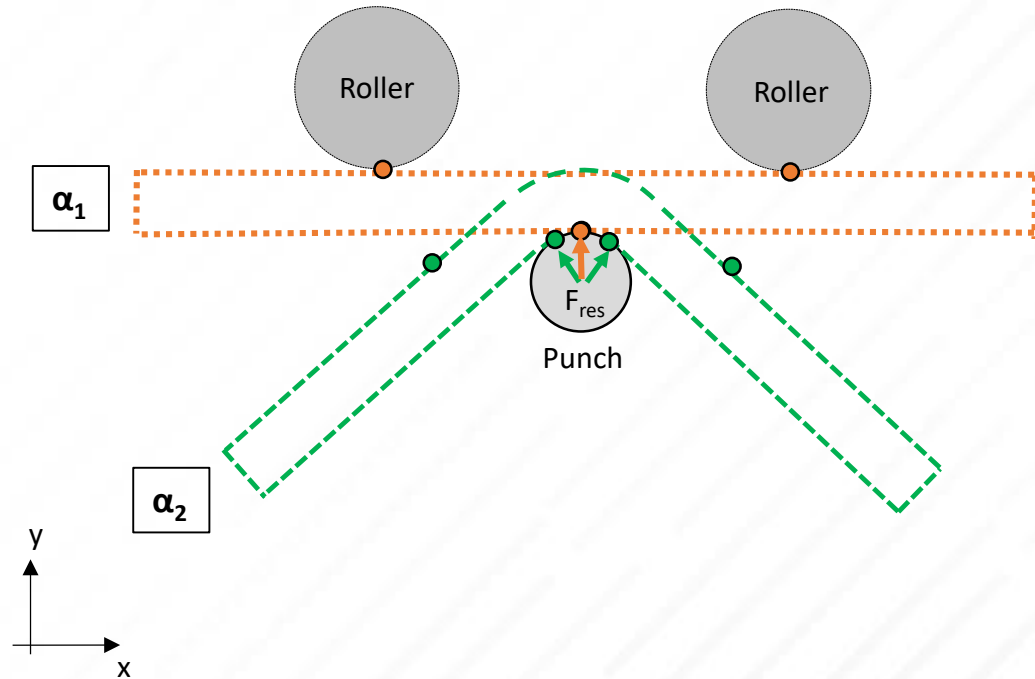
α_1

3-point bending



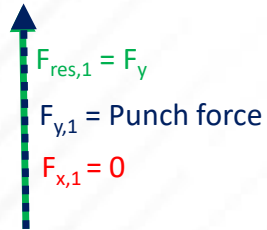
α_2

Transition 3-point \rightarrow 4-point bending



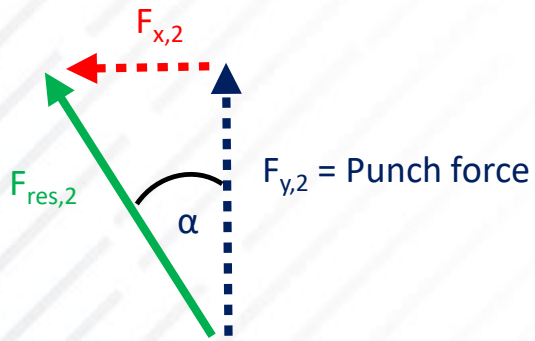
MECHANICS OF V-BEND TEST

What causes the load to reduce in the absence of fracture?



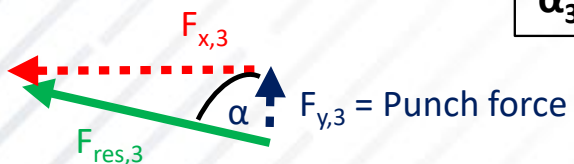
α_1

3-point bending



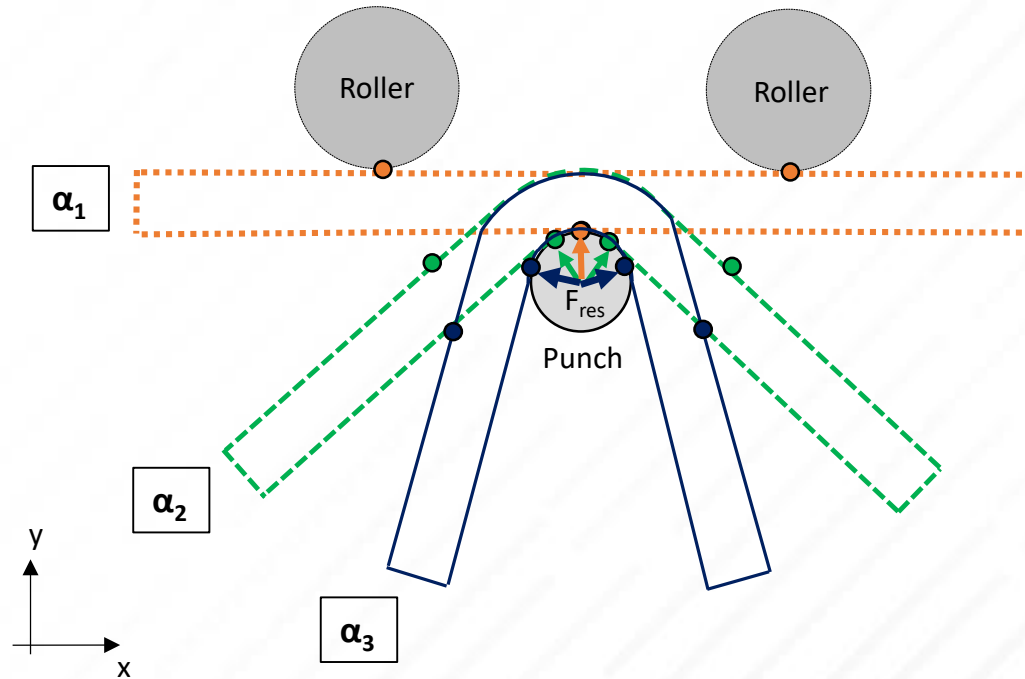
α_2

Transition 3-point → 4-point bending



α_3

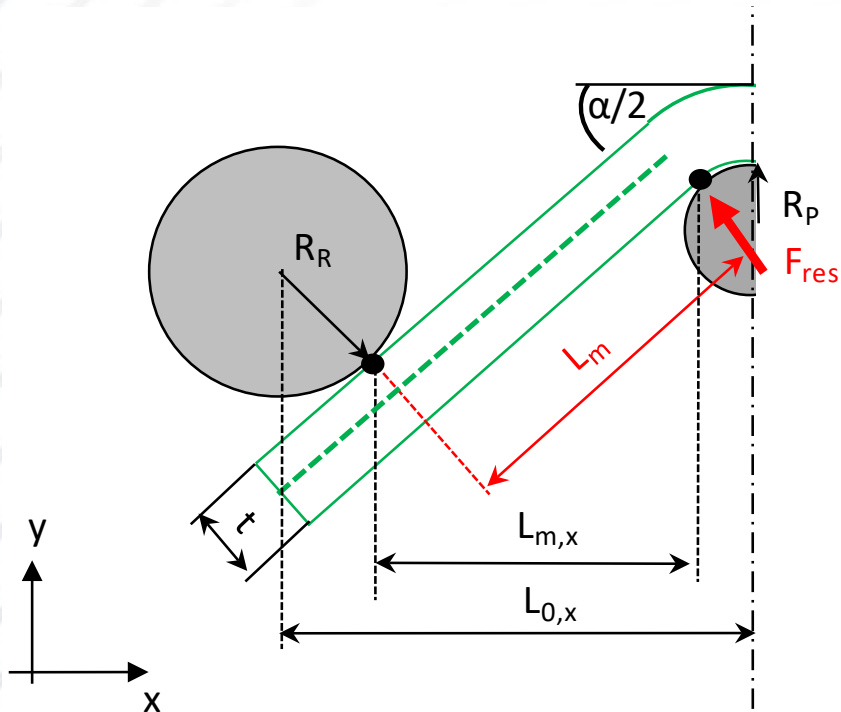
4-point bending



Punch force will drop eventually due to kinematic boundary conditions even without material rupture
 Not considered in the VDA 238-100 specification ...

BENDING MOMENT

Bending moment can be approximated from geometric considerations



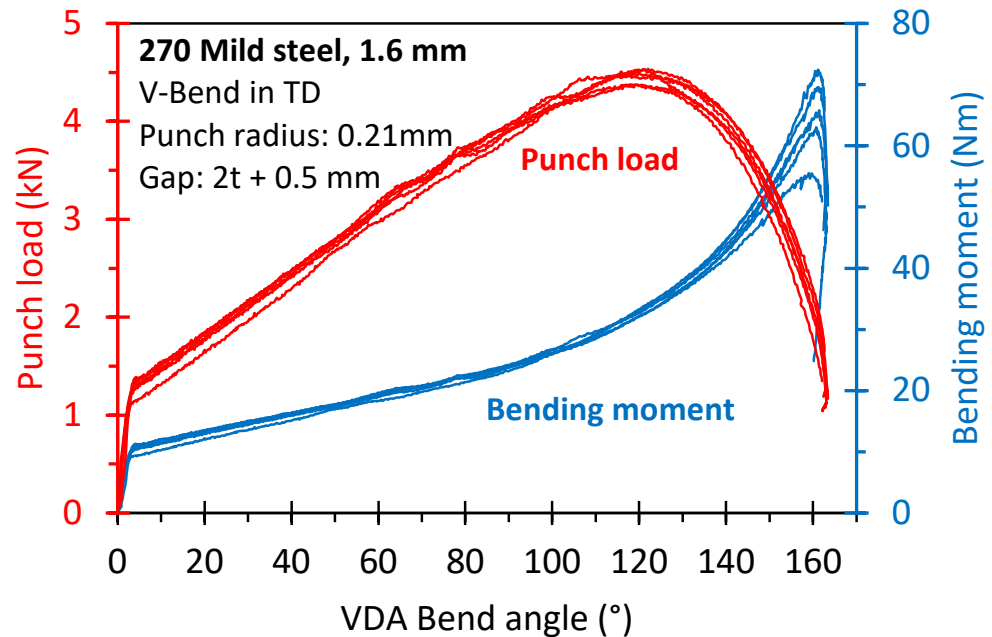
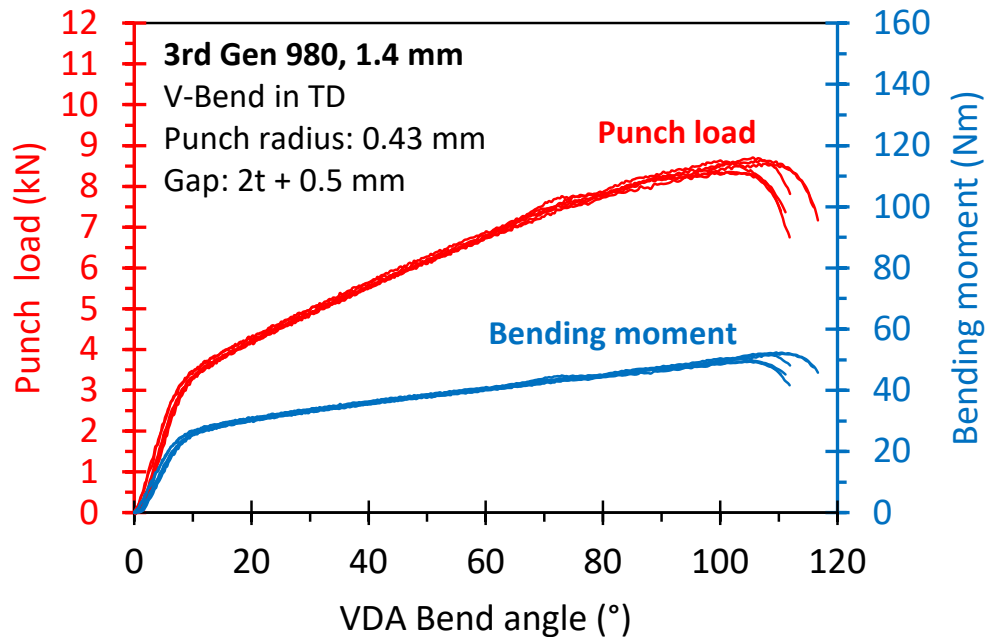
✓ Resultant force accounts for both the punch force and the tangential contribution

✓ Moment arm considers transition from 3-point to 4-point bending

$$M = F_{res} L_m = \frac{F_y}{2} \left(\frac{t + 0.25 + R_R - (R_R + R_P) \sin\left(\frac{\alpha}{2}\right)}{\cos^2\left(\frac{\alpha}{2}\right)} \right)$$

ADOPTION OF BENDING MOMENT

Adoption of bending moment works well for steel grades with clear fracture



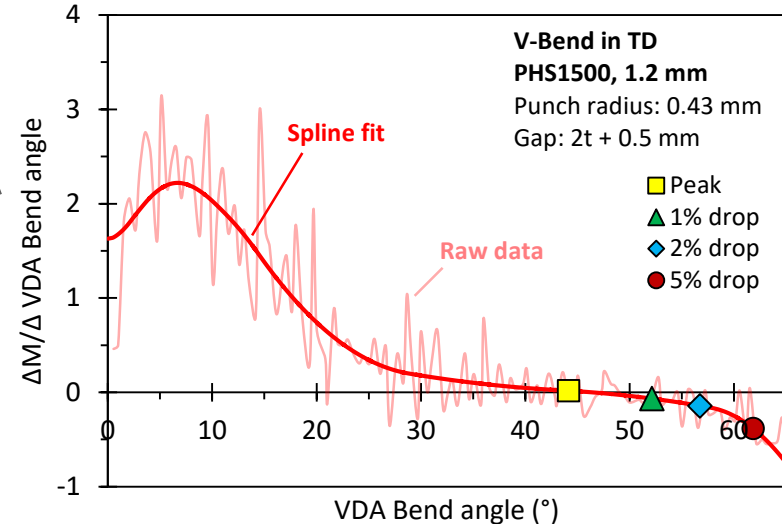
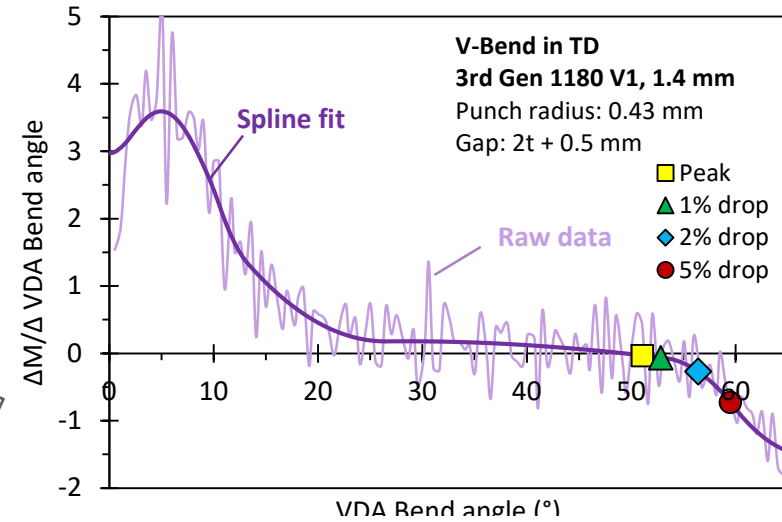
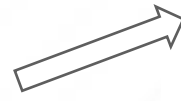
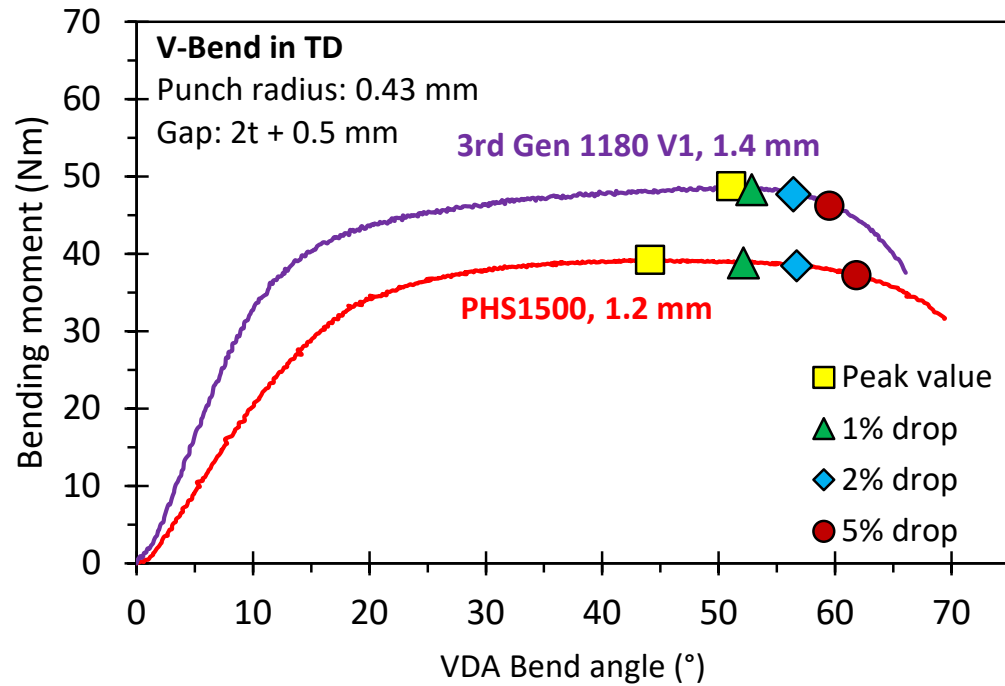
In the case of “false positives”, the bending moment provides remarkable improvement over the VDA 238-100 specification – *But drops at large bend angles ($>160^\circ$)*

CHALLENGES OF BENDING MOMENT

Low hardening materials have approximately constant bending moment

Incremental bending moment can have severe fluctuations about zero

Reliable identification of failure threshold is challenging



STRESS-BASED DETECTION METHOD

Bending moment is non-intuitive compared to punch force or stress

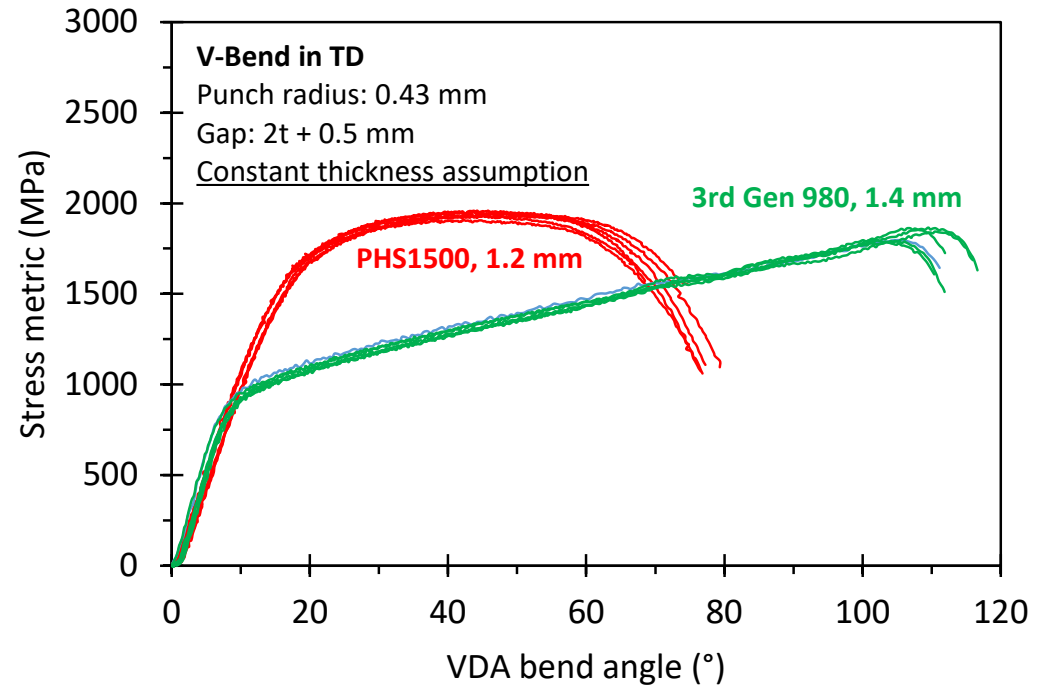
Stress integration of cross-section complex (load reversal, plasticity model, etc.)

Idea: Use closed-form solution for rigid, perfectly-plastic material to define stress metric

$$\Sigma = \frac{4}{t^2 w_0} M(F_y, \alpha)$$

t = nominal sheet thickness
 w_0 = specimen width

$$M_{\text{rigid, perfectly-plastic}} = \frac{\sigma_y t^2 w}{4} = \text{constant}$$



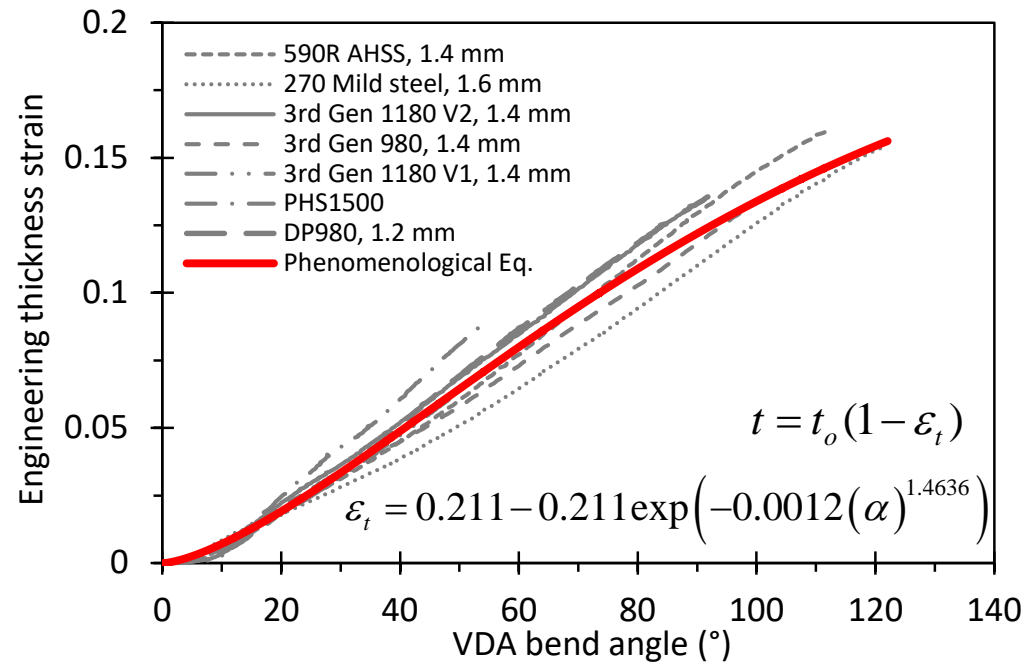
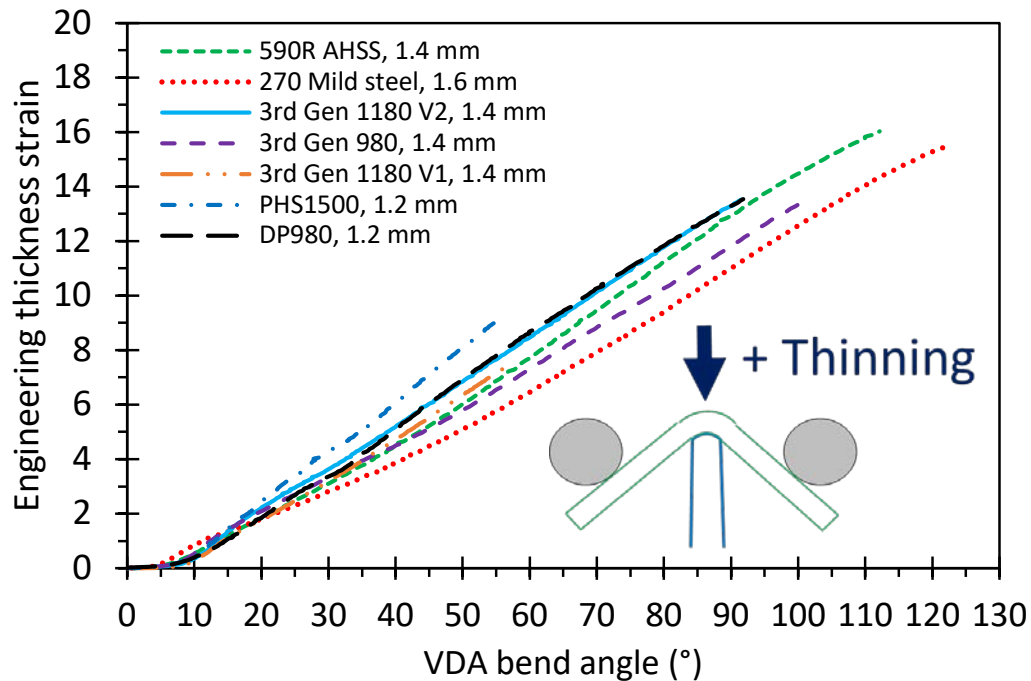
Improvement over bending moment but still challenges with low-hardening grades

Increase resolution by accounting for thinning of the cross-section

THINNING

V-bend frame at the University of Waterloo has a stationary punch

→ Thinning of the cross-section can be measured from out-of-plane displacement in DIC

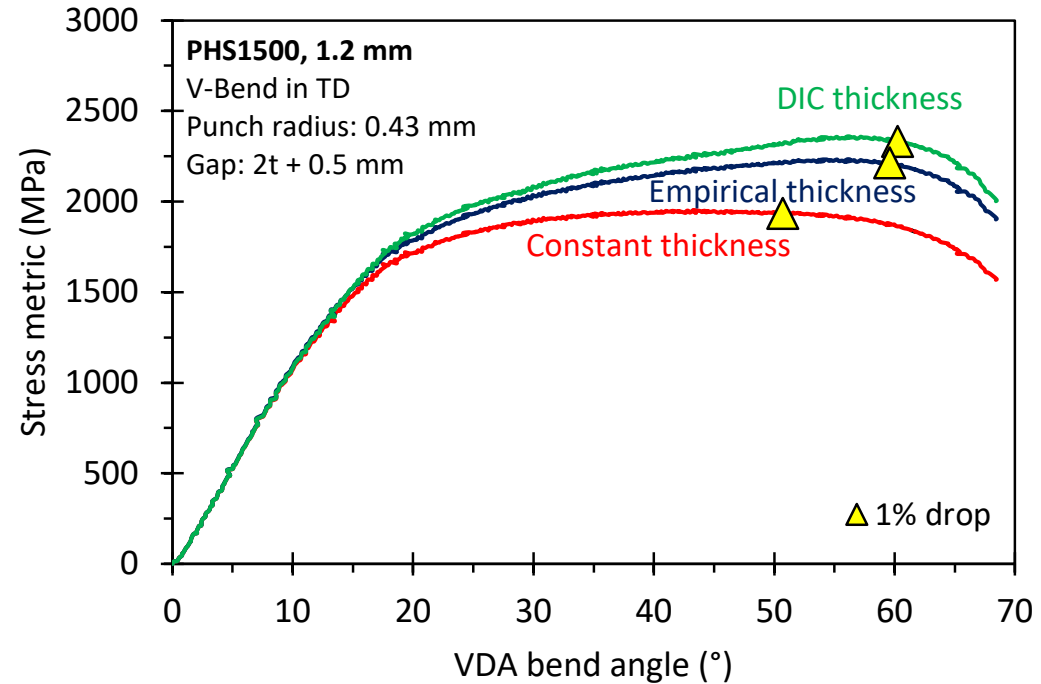
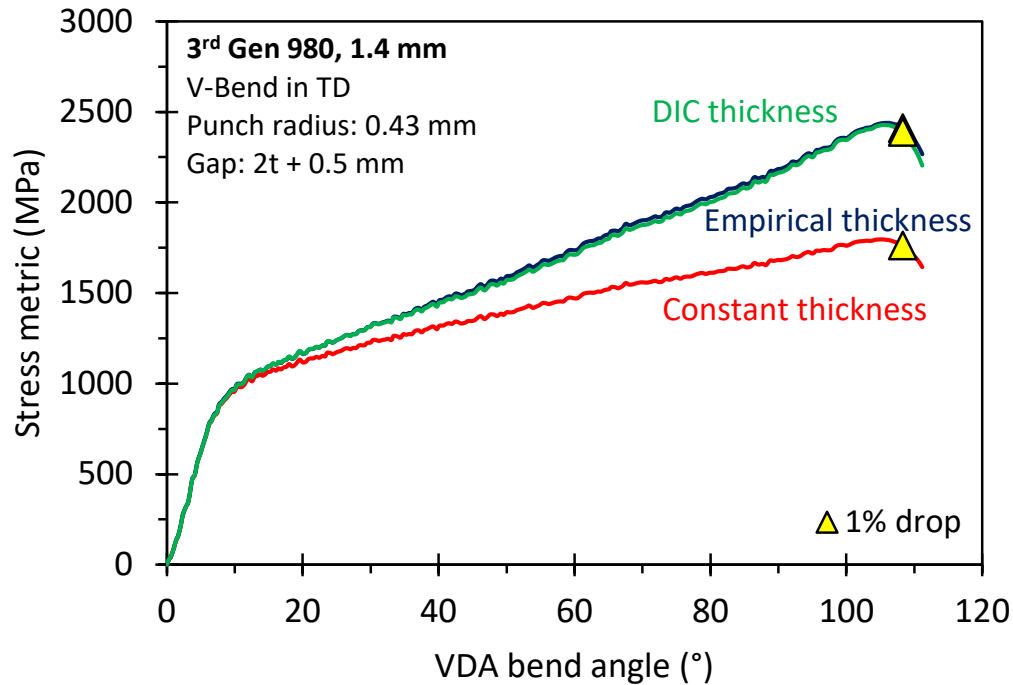


For VDA test frames without DIC, empirical fit for the engineering thinning strain

Future work: consider bend severity in empirical thinning equation

STRESS METRIC WITH THINNING

What is the effect of thinning upon the resolution of the stress metric?



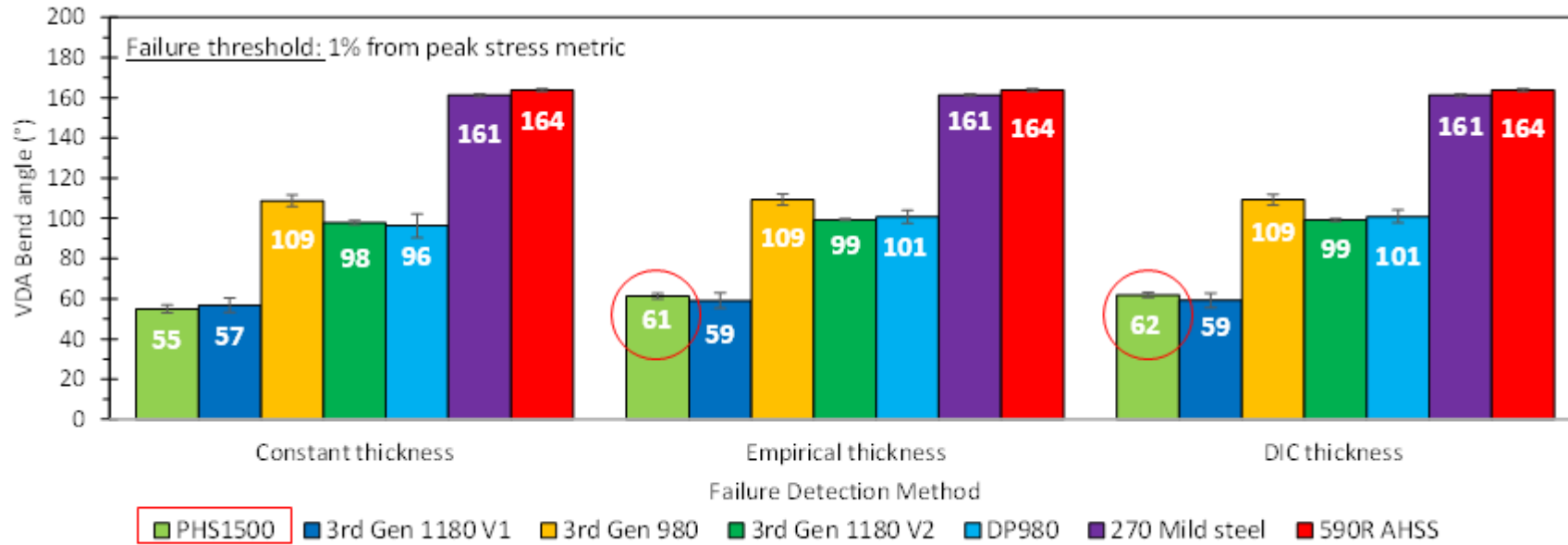
DIC thinning and empirical thinning method provide same fracture angle for high hardening 980 3rd Gen AHSS

Enhanced resolution for low-hardening PHS1500. Variation in stress metric magnitude but robust fracture detection

APPLICATION STRESS METRIC – BEND ANGLE

Comparison of recorded failure by the stress metric considering:

- (i) constant thickness
- (ii) empirical thickness
- (iii) instantaneous thickness from DIC

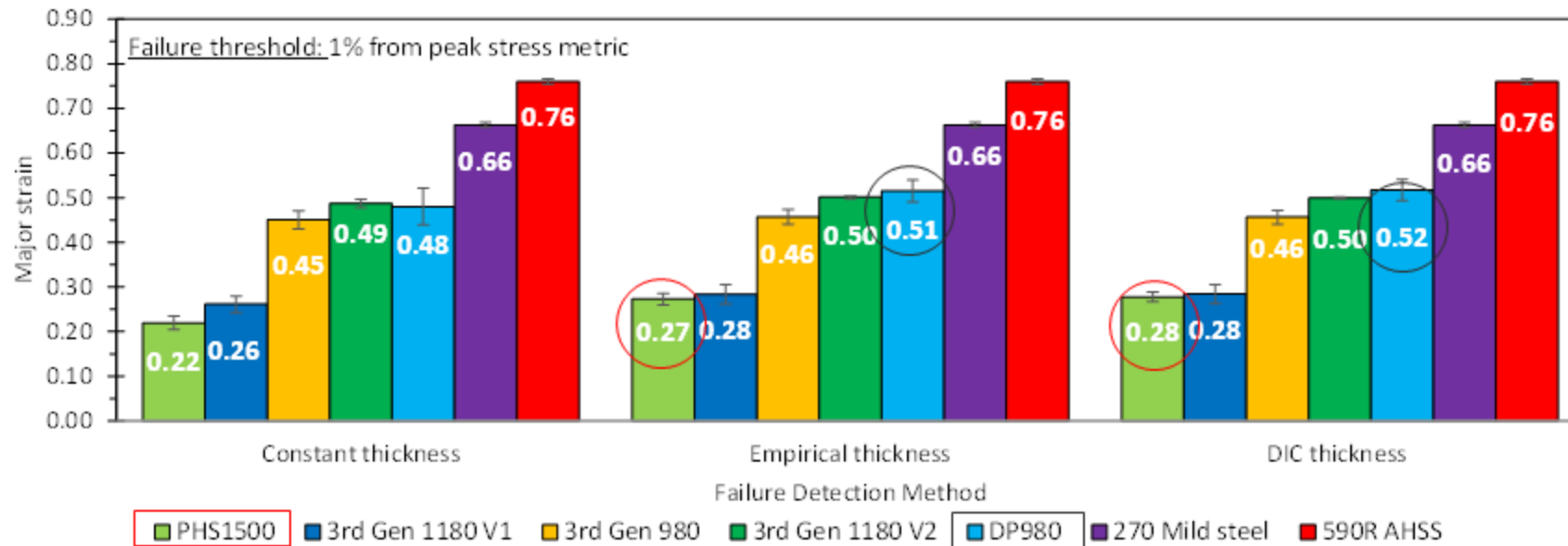


Maximum derivation of 1° when using the empirical thickness *versus* the thickness from DIC

APPLICATION STRESS METRIC – STRAIN

Good agreement between the empirical and the DIC thickness also reflected in the major strain

Max. deviation of 0.01 strain



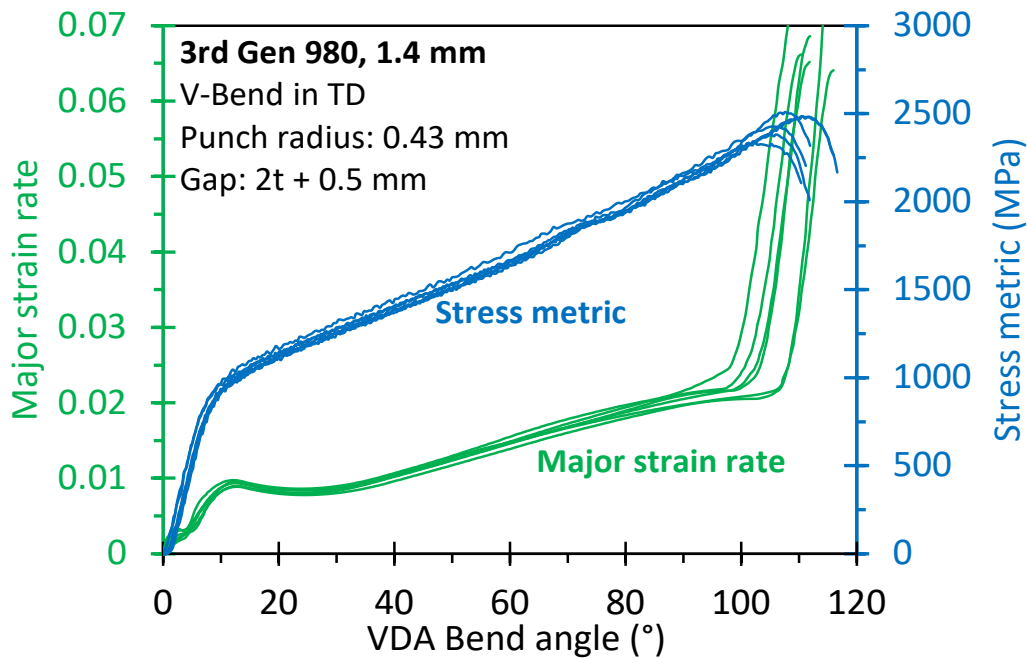
No additional complexity (no DIC required, no new parameters) introduced in stress metric but provides increased confidence to identify false positives

STRAIN-RATE BASED DETECTION METHOD

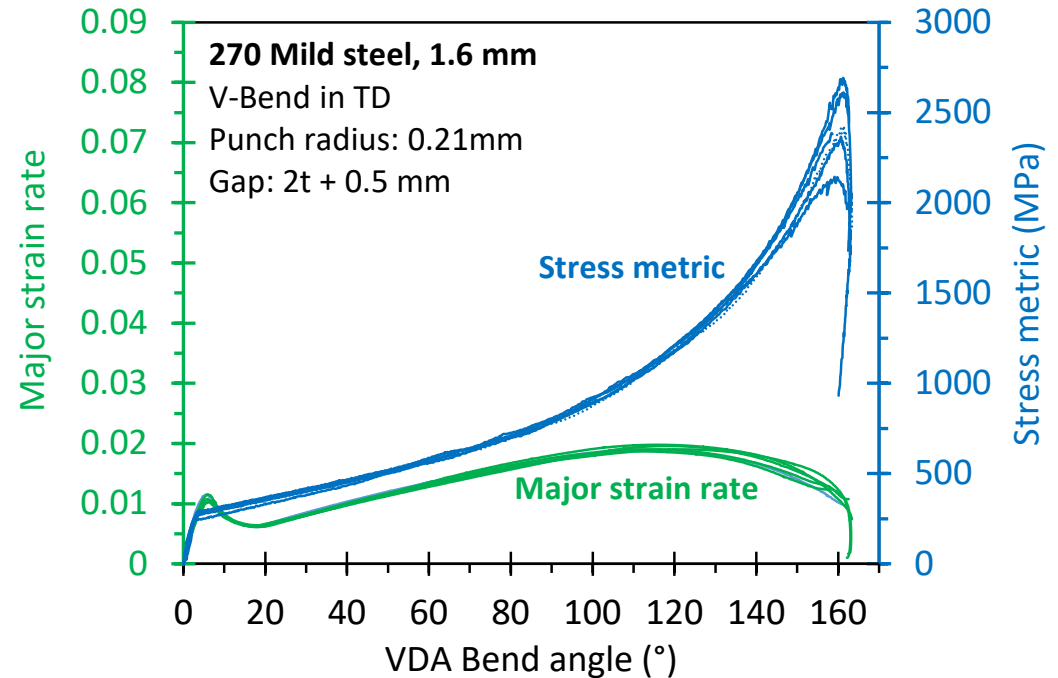
Stress metric remedied challenges encountered for steel grades with low hardening rate

Reduction in stress metric occurs at large bend angles ($>160^\circ$)

Consideration of the strain rate evolution since independent of punch force



In the case of fracture, strain accelerates



In the absence of fracture, strain rate decreases

MODIFIED LINEAR BEST FIT METHOD

Need criterion to detect abrupt acceleration (fracture) or deceleration (folding over)

Refine Linear Best Fit (LBF) Method by Volk and Hora (2011) for forming limit strains

(1) Unstable line fit: Least squares optimization

(2) Stable line fit

Start: Max. tensile strain on outer surface at onset of yielding

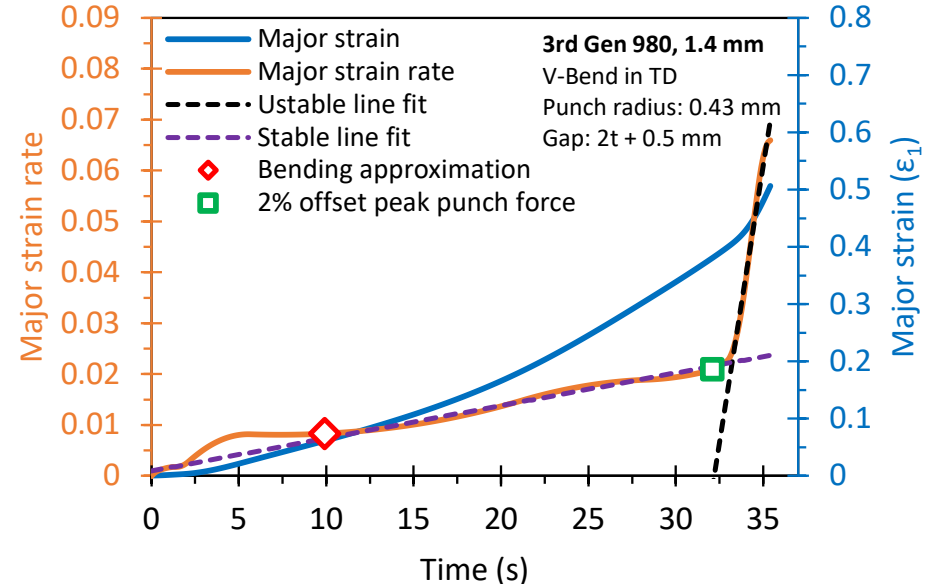
$$\epsilon_1^y \Big|_{R=R_o} \approx \ln \left(\frac{R_o}{R_m} \right) = \ln \left(1 + \frac{\kappa_y}{2} \right)$$

E = Young's Modulus
 v = Poisson's ratio
 σ_y = Yield stress
 κ_y = Rel. curvature

$$\kappa_y = \frac{t}{R_m} = 2\sqrt{1 - \exp(-2\epsilon_{el}^y)}$$

$$\epsilon_{el}^y = \frac{1 - v^2}{\sqrt{1 - v + v^2}} \frac{\sigma_y}{E}$$

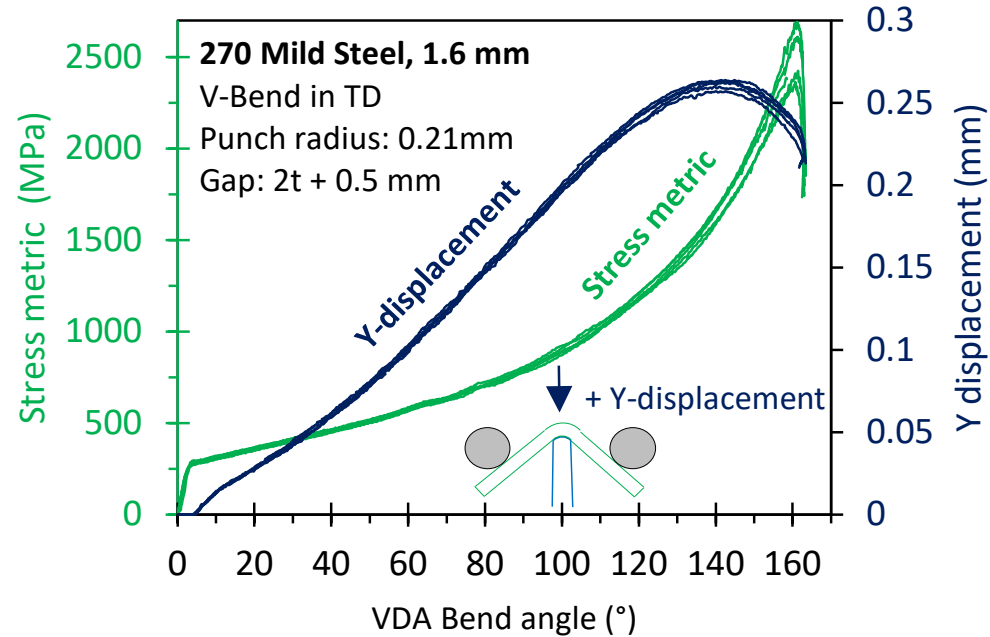
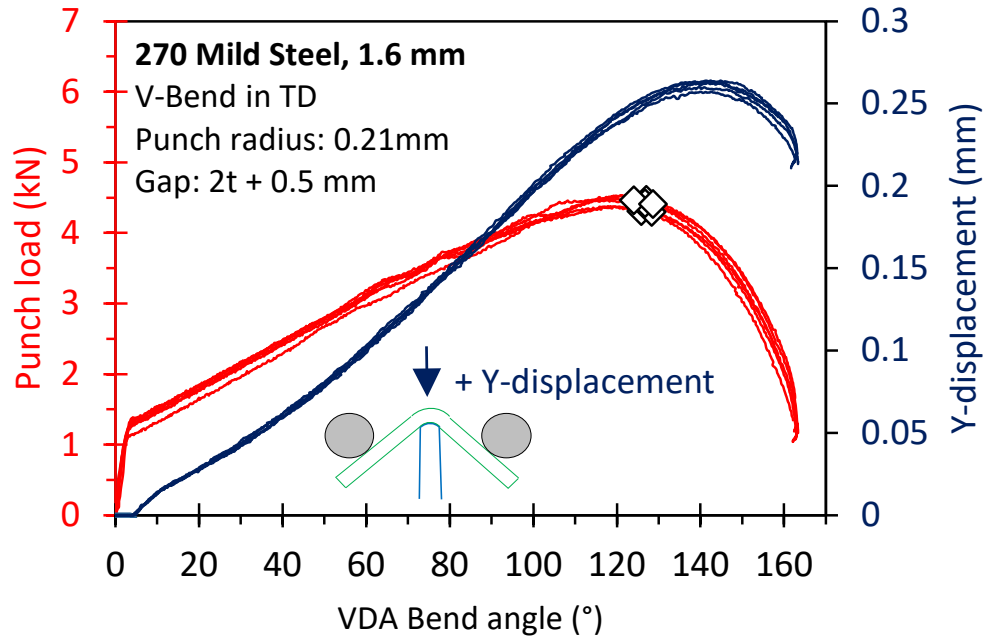
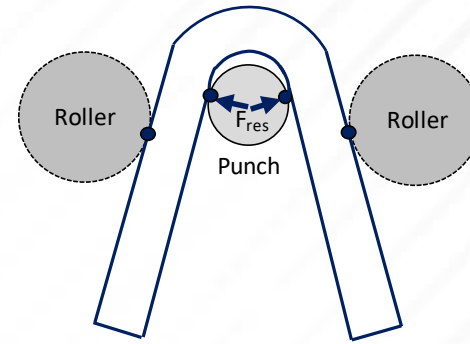
End: Corresponding strain rate at a 2% offset of peak punch force



PUNCH LIFT-OFF

Viable concern in the V-bend tests since inner bend radius no longer conforms to the punch tip radius

Out-of-plane displacement from DIC indicates when punch lift-off occurs

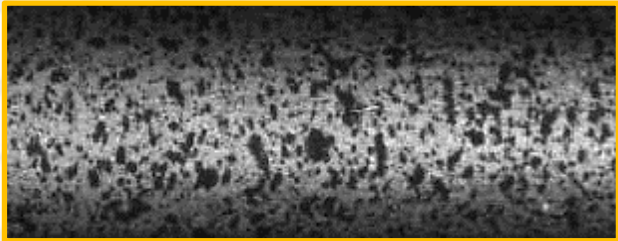


Punch force drops at a VDA bend angle of 127° whereas punch lift-off occurs at 144°

IDENTIFICATION OF FAILURE THRESHOLD

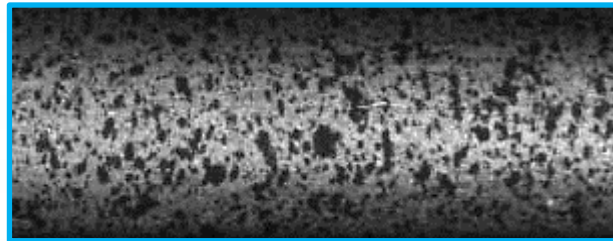
V-bend tests on 3rd Gen 980 without white background paint provide a direct view on specimen substrate surface

Mod. LBF Method



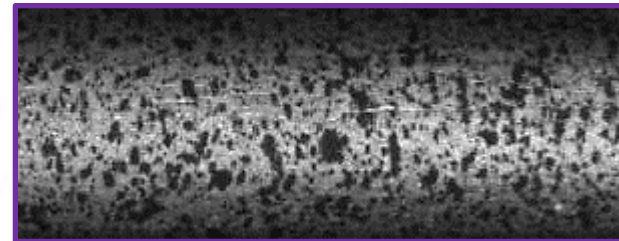
No hairline cracks

VDA 1% load drop



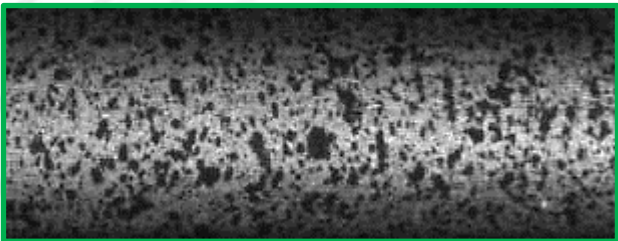
Hairline crack

Bending moment 1% drop



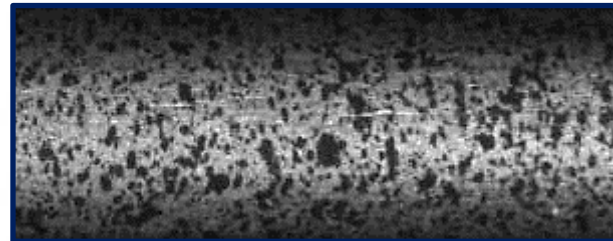
Minor cracks

VDA 60 N load drop



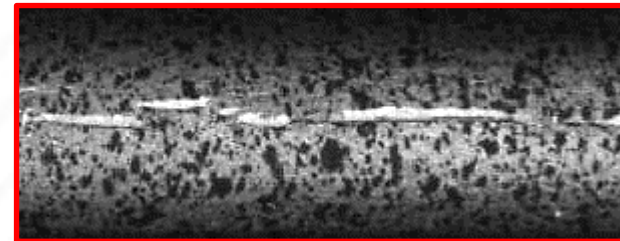
No hairline cracks

Stress metric 1% drop



Minor cracks

VDA 48% load drop



Cracks

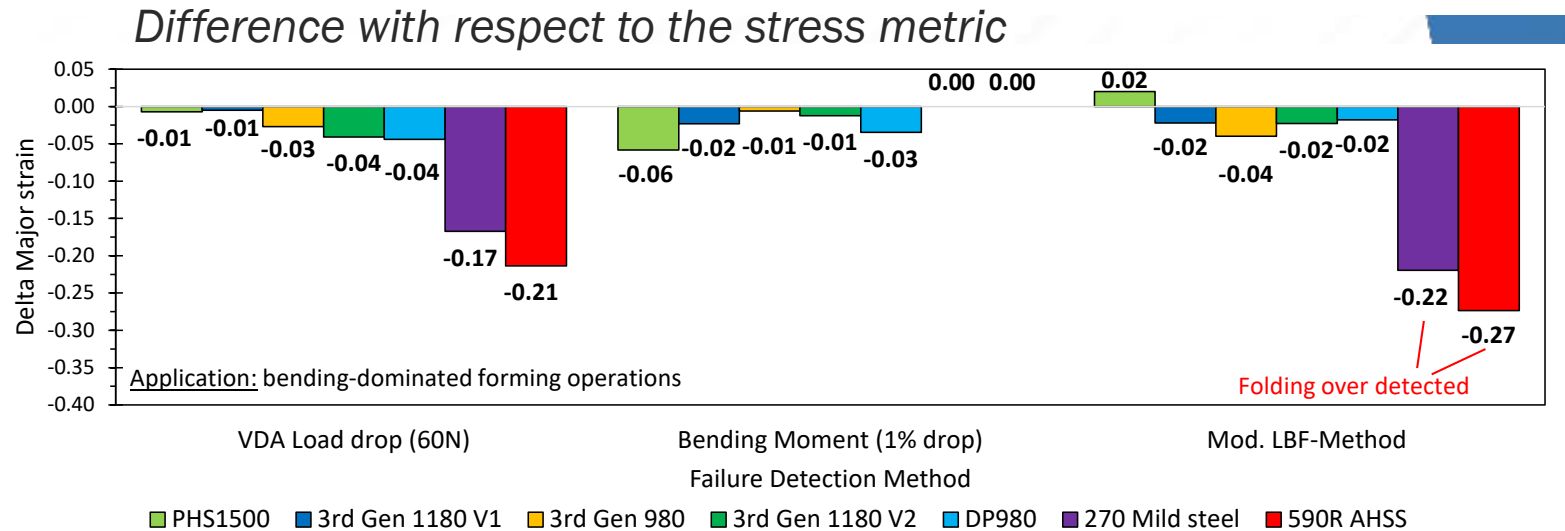
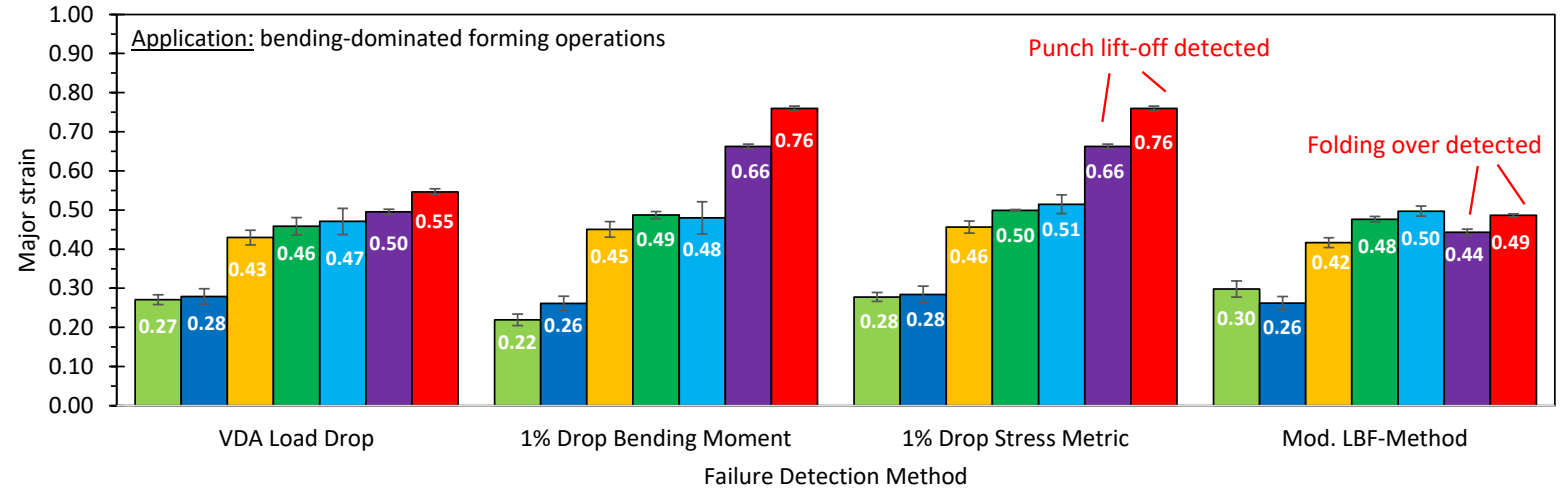
Threshold dependent upon application: bending-dominated forming operation or fracture?

COMPARISON OF FAILURE DETECTION METHOD

VDA 238-100 specification works well for high-strength steels with low bend angles (60°)

Bending moment works well for steel grades with appreciable hardening

Strain rate method is occasionally more conservative but can detect folding over



CONCLUSIONS

- For ductile steel grades or thin materials with low bend severity, reliance upon the punch force as unique fracture metric might lead to inconclusive results and require additional verification to confirm material failure
- Adoption of the bending moment-based failure metric provides some improvement over VDA 238-100 failure detection but selection of a robust failure threshold might be challenging for material with low hardening rates
- The stress-based failure metric accounts for thinning of the cross-section either through DIC or an empirical equation. No new parameters or DIC required.
- Consideration of the major strain rate can shed light into potential folding over
- Punch lift-off can be identified by tracking the out-of-plane displacement using DIC and was found to occur past the recorded drop in the punch force at VDA bend angles of about 145°

ACKNOWLEDGEMENTS



ArcelorMittal



FOR MORE INFORMATION

Jacqueline Noder
University of Waterloo
jnoder@uwaterloo.ca

Prof. Butcher
University of Waterloo
cbutcher@uwaterloo.ca

REFERENCES

1. Noder, J., Abedini, A., Butcher, C., (2020). Evaluation of the VDA 238-100 Tight Radius Bend Test for Plane Strain Fracture Characterization of Automotive Sheet Metals, *Experimental Mechanics*, 61.
2. Cheong, K., Omer, K., Butcher, C., George, R., Dykeman, J., (2017). Evaluation of the VDA 238-100 tight Radius Bending Test using Digital Image Correlations Strain Measurements, *IOP Conference Series: Journal of Physics*, 896
3. Troive L., (2017). New method for evaluation of bendability based on three-point bending and the evolution of the cross-section moment, *Journal of Physics Conference Series* 896(1).
4. Volk, W., Hora, P. (2011). New algorithm for a robust user-independent evaluation of beginning instability for the experimental FLC determination, *International Journal of Material Forming*, 4, 339-346.
5. Yu, T. X., Zhang, L. C., (1996). *Plastic Bending: Theory and Applications*, Series on Engineering Mechanics, 2, 572.
6. Noder, J., Dykeman, J., Butcher, C., (2020). New Methodologies for Fracture Detection of Automotive Steels in Tight Radius Bending: Application to the VDA 238-100 V-Bend Test, *Experimental Mechanics*, 61, 367-394.